Direct Measurement of Specific Membrane Capacitance in Neurons

Luc J. Gentet,* Greg J. Stuart,* and John D. Clements†
*John Curtin School of Medical Research and †Division of Biochemistry and Molecular Biology, Australian National University, Canberra, Australian Capital Territory 0200, Australia

ABSTRACT The specific membrane capacitance (C_m) of a neuron influences synaptic efficacy and determines the speed with which electrical signals propagate along dendrites and unmyelinated axons. The value of this important parameter remains controversial. In this study, C_m was estimated for the somatic membrane of cortical pyramidal neurons, spinal cord neurons, and hippocampal neurons. A nucleated patch was pulled and a voltage-clamp step was applied. The exponential decay of the capacitative charging current was analyzed to give the total membrane capacitance, which was then divided by the observed surface area of the patch. C_m was 0.9 μF/cm^2 for each class of neuron. To test the possibility that membrane proteins may alter C_m, embryonic kidney cells (HEK-293) were studied before and after transfection with a plasmid coding for glycine receptor/channels. The value of C_m was indistinguishable in untransfected cells and in transfected cells expressing a high level of glycine channels, indicating that differences in transmembrane protein content do not significantly affect C_m. Thus, to a first approximation, C_m may be treated as a "biological constant" across many classes of neuron.

INTRODUCTION

The outer membrane of nerve cells is composed of a lipid bilayer ~8–10 nm thick, which acts as a leaky capacitor. The capacitance per unit area of membrane is referred to as the specific capacitance (C_m), and is a fundamental parameter in models of the electrical properties of neurons (Rall, 1962; Jack et al., 1983). It plays an important functional role in synaptic integration and signal propagation. C_m and dendritic geometry together determine the amplitude of the postsynaptic potential at the site of a fast synaptic input. This is because the dendritic tree is depolarized when the brief synaptic current delivers charge to the local membrane capacitance. The charge then moves rapidly away from the synapse, carried by axial currents in the dendritic cytoplasm. The speed with which this signal is propagated to the soma is inversely proportional to C_m. An accurate estimate of this important functional parameter is therefore required to understand and to model a nerve cell's electrical behavior.

The specific membrane capacitance is determined by the thickness of the membrane and by its dielectric constant. These parameters are largely determined by the lipid constituents of the cell membrane, although they are also influenced by the protein content. Membrane constituents are broadly similar across different regions of the nervous system, so C_m has traditionally been viewed as a "biological constant" (Cole, 1968). This view neglects possible cell-to-cell differences in the density of proteins embedded in the membrane. At a sufficiently high concentration, embedded proteins will increase the average thickness and the dielectric constant of the membrane (Fernandez et al., 1982). For this reason, the value of C_m may not be precisely constant throughout the dendritic tree, or from neuron to neuron (Major et al., 1994; Thurbon et al., 1998; Chitwood et al., 1999).

Artificial lipid bilayers can be manufactured that contain no proteins, and C_m can be estimated with precision. Two typical values of C_m are 0.70 μF/cm^2 for bilayers formed with asolectin lipids and 0.94 μF/cm^2 for membranes prepared from egg lecithin (Niles et al., 1988). Early estimates of C_m for biological membrane were obtained using the squid giant axon preparation. The large diameter of this axon permits membrane surface area and capacitance to be measured directly, and C_m was estimated to be 1.0–1.3 μF/cm^2 (Curtis and Cole, 1938; Hodgkin and Huxley, 1952). More recently, mice mast cells were studied using whole-cell patch clamp, and C_m was found to be 1.0 μF/cm^2 (Solsona et al., 1998). An independent estimate of C_m for spherical cultured mammalian cells has been obtained using the electro-rotation technique. Suspended cells are subjected to an oscillating electric field, which causes them to spin. The rate of rotation is measured and used to estimate C_m. A value of 0.8 μF/cm^2 was obtained for three different cell lines (Sukhorukov et al., 1993).

It is more difficult to measure C_m in neurons because of their complex morphology. The traditional approach has been to record the electrical response to small current or voltage steps applied at the soma, then to stain the neuron with an intracellular dye and reconstruct its detailed morphology. The morphology is used to construct a "compartmental" model that can simulate the electrical response of the cell to the applied current or voltage steps. The free parameters of this model, which include C_m, are adjusted to optimally fit the simulated response to the recorded response. This relatively complex and indirect approach has yielded a wide range of values for C_m. Recent estimates include 0.75 μF/cm^2 in hippocampal pyramidal neurons (Major et al., 1994), 2.4 μF/cm^2 in spinal cord ventral horn

Received for publication 13 December 1999 and in final form 21 March 2000.

John Clements, Division of Biochemistry and Molecular Biology, Australian National University, Canberra, ACT 0200, Australia Tel.: 61-2-6249-3465; Fax: 61-2-6249-0313; E-mail: john.clements@anu.edu.au.

0006-3495/00/07/314/07 $2.00

neurons (Thurbon et al., 1998) and 0.9 μF/cm^2 in hippocampal interneurons (Chitwood et al., 1999). This range may reflect real differences in C_m between different cell types, or alternatively may be due to the inherent difficulty in estimating C_m in cells with complex morphology.

In this study we used a simpler, more direct approach for measuring C_m. A nucleated patch was pulled from a neuron and the capacitance and surface area of this simplified structure were measured. C_m was measured using this approach in several different classes of neuron. We also tested whether expression of a high density of membrane proteins in HEK-293 cells altered C_m.

METHODS

Brain and spinal cord slice

Slices were obtained from layer 5 of the cortex (300 μm thick) or from the lumbar region of the spinal cord (400 μm thick) of 7–14-day-old Wistar rats. Cells were visualized using differential interference contrast (DIC) infrared microscopy.

Cell culture

Hippocampal neurons were dissociated and grown on glass coverslips as previously described (Furshpan et al., 1986; Bekkers and Stevens, 1991). Cells were used after 7–16 days in culture. HEK-293 cells were grown in continuous culture as previously described (Rajendra et al., 1994). They were suspended then plated on plastic coverslips coated with rat tail collagen and poly-D-lysine. Recordings were made from 1 to 3 days after plating. A subset of the cells was transfected by electroporation Gene Pulser (Bio-Rad, Hercules, CA) at 250 V, 500 μF or 960 μF, before plating. The width of the pulse was typically 10–15 ms, and the transfection rate was 2–10%.

Electrophysiology

Currents were recorded using an Axopatch 200A amplifier (Axon Instruments, Foster City, CA). Data were low-pass-filtered at 50 kHz and recorded at 100–200 kHz. Recording pipettes were made of borosilicate glass and were coated with sylgard. After fire-polishing, the pipette resistance was 2–3 MΩ for experiments performed on HEK-293 cells and 4–6 MΩ for experiments performed on neurons and glial cells. Series resistance was not compensated. Pipette capacitance was fully compensated while in the cell-attached configuration. The internal solution of the patch pipette contained 150 mM CsCl, 10 mM HEPES, 10 mM EGTA, pH 7.4, and osmolarity was adjusted to 300–310 mOsm with sorbitol. HEK-293 cells were continuously perfused with a bath solution containing 140 mM NaCl, 5 mM KCl, 2 mM $CaCl_2$, 1 mM $MgCl_2$, 10 mM glucose, 10 mM HEPES, pH 7.4, with osmolarity adjusted to 310 mOsm with sorbitol. Cultured neurons and glial cells were perfused with a bath solution containing 135 mM NaCl, 5 mM KCl, 3 mM $CaCl_2$, 10 mM glucose, 10 mM HEPES, pH 7.3, with osmolarity adjusted to 310 mOsm with sorbitol. Brain slices were perfused with a bath solution containing 125 mM NaCl, 3.0 mM KCl, 1.25 mM NaH_2PO_4, 25 mM $NaHCO_3$, 1 mM $MgCl_2$, 2 mM $CaCl_2$, 25 mM glucose bubbled with 95% O_2/5% CO_2 (pH 7.4).

Nucleated patches were pulled from cortical pyramidal cells and spinal cord neurons in slice preparations, and from hippocampal neurons and glial cells in culture. They were lifted close to the surface of the bath (~200 μm) to reduce the pipette capacitance (Fig. 1 *A*). A −5 mV pulse was applied from a membrane potential of −60 mV and 100–200 capacitative transients were recorded and averaged. At the end of the recording, the patch was ruptured and the open tip of the pipette was pressed against a small sylgard ball, resulting in a GΩ seal (Fig. 1 *B*). The depth of the pipette in the bath solution was not changed. Again, a −5 mV pulse was applied and the transient, which was due to charging of the residual uncompensated pipette capacitance, was averaged. The residual capacitance transient was subtracted from the capacitative transient recorded from the nucleated patch.

HEK-293 cells were lifted from the bottom of the coverslip using a patch electrode in the cell-attached configuration. The pipette capacitance was fully compensated before rupturing the patch and obtaining a whole-cell recording. A −5 mV voltage pulse was applied from a membrane potential of −20 mV and 100–200 capacitative transients were averaged. The cells were deliberately expanded by applying sustained positive pressure (20–50 mm Hg) via the recording electrode, and additional transients were recorded.

Some of the HEK-293 cells were cotransfected with two different plasmids encoding the wild-type alpha-1 human glycine receptor subunit and the CD4 cell surface antigen. The transfected cells were identified using Dynabeads (Dynal. Oslo, Norway) coated with CD4 antibody (Jurman et al., 1994).

Analysis of the capacitative transient

A simplified circuit can be used to describe the nucleated patch or whole-cell recording configuration (Fig. 1, *C* and *D*). The simplification requires that the patch membrane is isopotential, and that no voltage-dependent conductances are active. This model circuit predicts that the current transient following a step in the voltage-clamp command potential will have an exponential time course. The amplitude, decay time constant, and steady-state level of this transient can be analyzed to estimate the series resistance of the recording pipette (R_s), the patch (or cell) membrane resistance (R_p), and membrane capacitance (C_p).

$$R_s = V_{step}/I_{peak} \quad (1)$$

$$R_p = V_{step}/I_{ss} - R_s \quad (2)$$

$$C_p = \tau(1/R_s + 1/R_p) \quad (3)$$

where V_{step} is the amplitude of the voltage-clamp step, I_{peak} is the peak amplitude of the current transient immediately after the step is applied, τ is the decay time constant of the current, and I_{ss} is the steady-state current at longer times following the step. The parameters τ, I_{peak}, and I_{ss} were determined by fitting a single exponential function with an added constant to the current transient recorded during the voltage step. This method for estimating C_p was tested by attaching a model cell (two resistors and a capacitor in the configuration shown in Fig. 1 *D*) to the patch clamp amplifier headstage. It was found that the first one or two sample points (~10 μs) in the current transient were sensitive to the fast pipette capacitance compensation setting, so these points were not included in the exponential fit. The pipette capacitance can change during an experiment due to changes in the depth of the bath, or in the shape of the meniscus around the patch electrode. The value of I_{peak} was determined by extrapolating the fitted exponential curve back to the start of the current response. The method accurately estimated the capacitance of the model cell. An alternative approach for estimating membrane capacitance by integrating the total current transient during the voltage step was also tested, but it was found to be more sensitive to changes in pipette capacitance.

Estimation of the membrane surface area of nucleated patches

The dimensions of nucleated patches were measured by DIC infrared microscopy from images captured at high magnification (40× objective

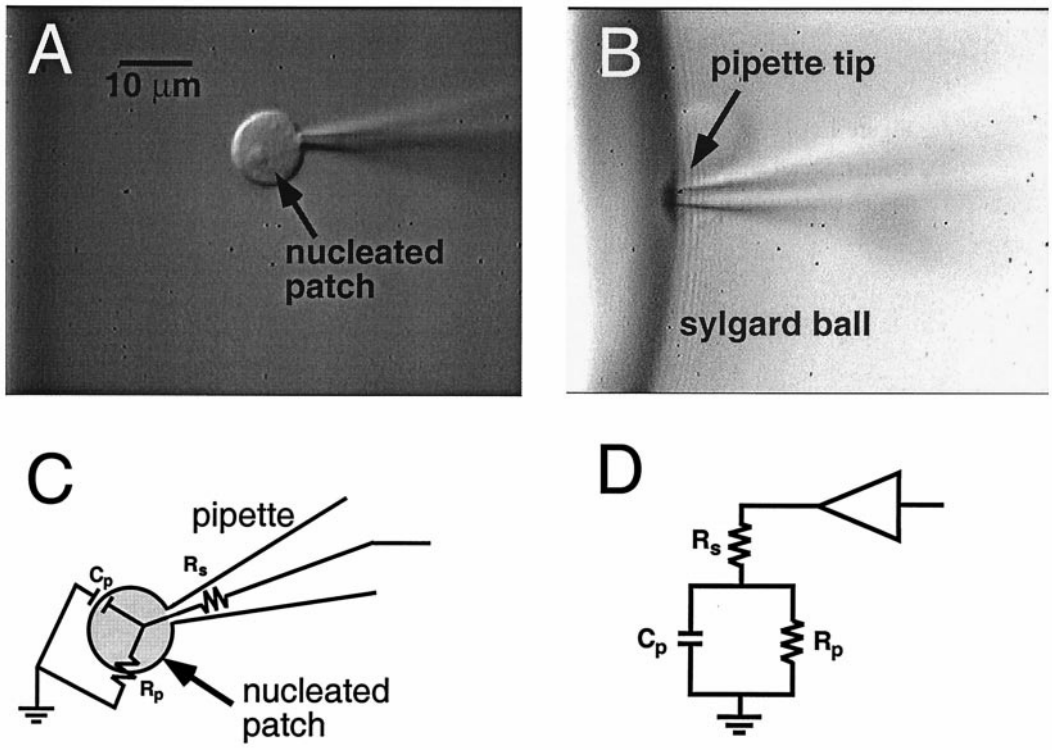

FIGURE 1 (*A*) A nucleated patch from a cortical pyramidal neuron visualized using differential interference contrast (DIC) infrared microscopy. (*B*) A patch electrode is pressed against a small sylgard ball creating a GΩ seal. This configuration is used to record the current transient due to uncompensated electrode capacitance. (*C*) Schematic diagram of the nucleated patch recording configuration showing the equivalent elements. (*D*) The equivalent circuit used to describe the nucleated patch recording configurations. R_s: series resistance of the electrode; R_p: patch membrane resistance; C_p: patch membrane capacitance.

coupled with a 4× magnification lens) by a video camera mounted on the microscope (Fig. 1 *A*). Minor and major axes were measured. It was assumed that the patches were approximately ellipsoid, and the membrane surface area was calculated using the following formula:

$$\text{Surface area} = (\text{major axis} + \text{minor axis})^2\,(\pi/4) \qquad (4)$$

Estimation of the membrane surface area of HEK-293 cells

The dimensions of HEK-293 cells were measured by phase-contrast microscopy using a 40× objective and an eyepiece graticule. Major and minor axes were measured and the apparent surface area was estimated using Eq 4. The measurements were repeated after the HEK-293 cell was expanded by applied pressure. HEK-293 cells have many fine processes (Fig. 2) and the presence of filopodia may explain the ability of these cells to expand in response to internal pressure. Pressure was applied in an attempt to flatten out the filopodia and permit a more accurate estimate of total membrane surface area under light microscopy.

When HEK-293 cells were observed under an electron microscope, it was revealed that they possess many fine processes or filopodia that are not visible under a light microscope (Fig. 2 *A*). For electron microscopy studies, HEK-293 cells were fixed in 2% gluteraldehyde in a 0.1 M sodium cacodylate buffer (pH 7.4) for two hours, then postfixed in 1% osmium tetroxide for 1 hour. Cells were stained en bloc in 2% uranyl acetate in either a pellet form or on a coverslip, dehydrated in ethanol, and embedded in resin at 70°C overnight. Coverslips were removed by dipping in liquid nitrogen and cells were sectioned using a diamond knife and photographed under a transmission electron microscope.

It was necessary to adjust the surface area of HEK-293 cells estimated by light microscopy to take account of the fine processes revealed in electron micrographs. The adjustment factor was calculated as follows. Electron micrographs were digitally processed (NIH Image, National Institutes of Health, Washington, DC) to form an outline of a cell. The image was converted into binary form by thresholding, then expanded and eroded three or four times to fill gaps in the cell's membrane outline (Fig. 2 *B*). Any processes that were touching each other to form a closed loop in the binary image were manually separated. The membrane surface area was measured from the micrographs in two ways. The first method ignored all processes and treated the cell as a smooth ellipsoid. Major and minor axes were measured and Eq. 4 was used to estimate the membrane surface area (Fig. 2 *B*). The value obtained by this method is obviously an underestimate, but it is comparable to the value obtained by light microscopy during electrophysiological experiments (see above). The second method used NIH Image to measure the perimeter of the cell, including its processes. The following formula was then used to estimate the total membrane surface area of a cell:

$$\text{Total surface area} = \text{perimeter}^2/\pi \qquad (5)$$

A few fine processes were lost during the automated image enhancement, so this approach may slightly underestimate the membrane surface area. The ratio of the membrane surface areas obtained with these two methods was used to adjust the surface area of HEK-293 cells measured with light microscopy (see Results). All results are presented as mean ± SEM.

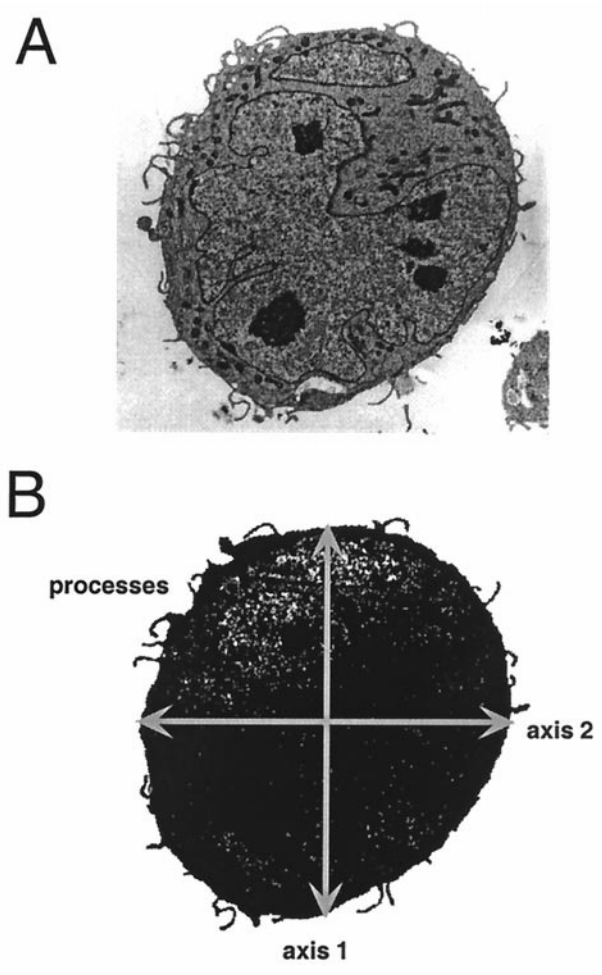

FIGURE 2 (*A*) Electron micrograph of an HEK 293 cell. (*B*) The same cell after processing with NIH Image. The micrograph was converted from gray-scale to binary by applying a threshold. Gaps in the cell perimeter were then filled in, and overlapping filopodia were separated. The two major axes were measured (*gray lines*).

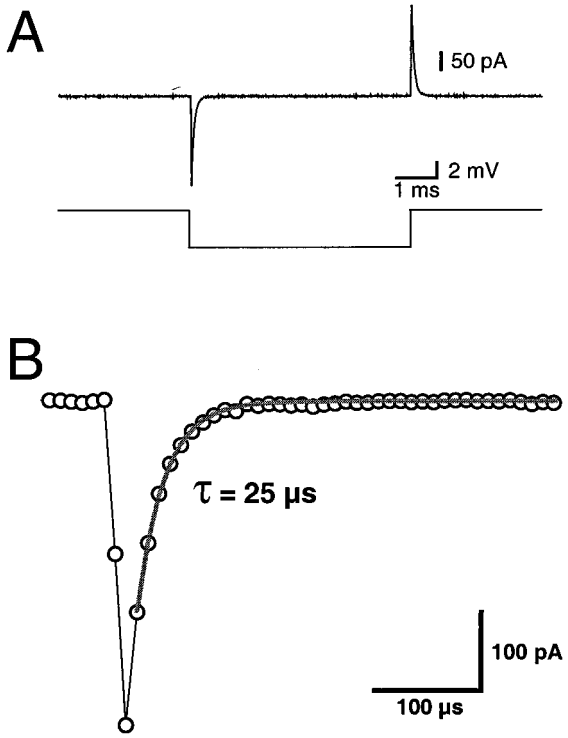

FIGURE 3 (*A*) The current transient recorded from a nucleated patch during a −5 mV voltage-clamp pulse at a sample rate of 100 kHz. The patch was pulled from a cortical pyramidal neuron. The transient is the ensemble average of 100 responses. (*B*) Expanded section of the current shown in (*A*) (*open circles*). An exponential function with an added constant was fit to the initial capacitative transient (*gray line*). The time constant of the fitted function was 25.2 μs.

RESULTS

Specific membrane capacitance of neurons and glial cells

Nucleated patches were pulled from the soma of cortical pyramidal neurons and spinal cord neurons in slice, and from hippocampal neurons and glial cells in culture. Glia were identified by the absence of a Na^+ current spike during voltage-clamp steps to 0 mV. Nucleated patches were clamped at −60 mV, steps of −5 mV were applied, and the ensemble average of the current response was determined. A typical transient recorded in a nucleated patch from a cortical pyramidal neuron is shown in Fig. 3. The average transient from each patch was fit with a single exponential function with an added constant, and the time constant and amplitude parameters were used to estimate R_s, R_p, and C_p (see Methods). The fit was rejected if the estimated value of R_s was less than the pipette resistance measured before the start of the recording. The data were also rejected if R_p was <500 MΩ, to exclude cases where the seal had degraded and become leaky. The value of C_p was divided by the measured surface area of the nucleated patch to calculate C_m. The values that were obtained for C_m for the various cell types are given in Table 1.

Increased membrane protein content does not alter C_m

It has been suggested that the protein content of biological membranes can significantly influence C_m by altering the

TABLE 1 C_m for nucleated patches

Cell type	C_m (μF/cm^2)
Cortical pyramidal neuron	0.92 ± 0.05 (n = 9)
Spinal cord neuron	0.85 ± 0.07 (n = 8)
Cultured hippocampal neuron	0.92 ± 0.08 (n = 7)
Cultured glial cell	1.06 ± 0.16 (n = 7)

The values obtained for C_m were similar across all cell classes. The average value across all neurons was 0.90 ± 0.03 ($n = 24$).

average dielectric properties of the membrane (Thurbon et al., 1998). To test this possibility, we measured C_m in transfected and untransfected HEK-293 cells. These cells are known to have few endogenous membrane ion channels, but after transfection they express high levels of ligand-gated ion channels and other membrane proteins (Rajendra et al., 1994). One group of HEK-293 cells was co-transfected with two different plasmids coding for the alpha-1 human GlyR and for the CD4 surface antigen. A second group of cells was not transfected, or was subjected to electroporation in the absence of plasmids (sham-transfected). In the transfected cells, the average steady-state current elicited by bath application of 1 mM glycine was 3.0 ± 0.7 nA ($n = 12$) at a holding potential of -20 mV (equivalent to 9 nA at -60 mV). This is larger than the steady-state current recorded in large adult neurons in response to bath application of glycine (Tapia and Aguayo, 1998; Ye et al., 1999), and confirms that the membrane density of GlyRs in the relatively small HEK-293 cells equaled or exceeded physiological densities of receptor protein. In addition, the HEK-293 cells expressed CD4 membrane protein at a high level.

HEK-293 cells were clamped at -20 mV, steps of -5 mV were applied, and the ensemble average of the current response was determined. Average capacitative transients were obtained from transfected and untransfected cells. A second series of membrane potential steps was delivered after each cell had been expanded by application of internal pressure (10–20 mm Hg). Pressure was applied in an attempt to flatten out any filopodia and permit a more accurate estimate of total membrane surface area under light microscopy. There was no detectable change in the capacitative transients after the cells were expanded, indicating that no extra membrane had been recruited (Fig. 4 *A*). The decay phase of the transient could be well-fitted with a single exponential (Fig. 4 *A*), indicating that the simplified three-element circuit (Fig. 1 *D*) provides an adequate description of these cells. The transients were analyzed by fitting an exponential function with added constant, and estimates of R_s, R_p, and C_p were obtained. In this context, C_p represents the whole-cell capacitance.

To calculate C_m, an estimate of membrane surface area is required. This was complicated by the many fine processes or filopodia that HEK-293 cells normally possess (Fig. 2). Two independent estimates of surface area were obtained. The first was based on the maximum diameter of the expanded cells measured under light microscopy after application of internal pressure. This approach assumes that all filopodia have been flattened out by the applied pressure. The second estimate was based on the initial diameter of the cells multiplied by a correction factor to account for the extra membrane due to small processes or filopodia, which was calculated from electron micrographs (see Methods).

The increase in the apparent diameter of each HEK-293 cell produced by internal pressure is indicated in Fig. 4 *B*.

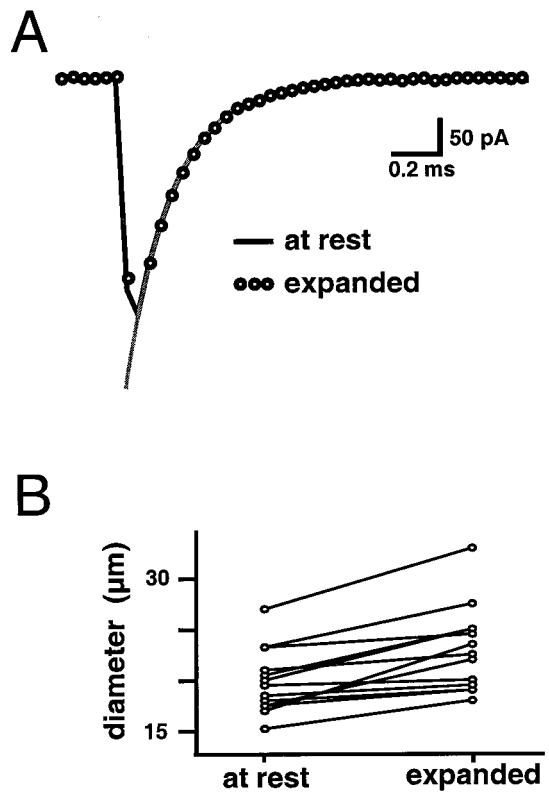

FIGURE 4 (*A*) Averaged capacitative transient in an untransfected HEK-293 cell before and after it was expanded by application of pressure. An exponential function was fit to the decay phase (*gray line*). (*B*) The increase in apparent diameter of individual HEK-293 cells induced by application of internal pressure ($n = 13$).

The average diameter increase was $11.2 \pm 2.2\%$ ($n = 13$), which corresponds to an increase in apparent surface area of $38 \pm 7\%$. In contrast, analysis of electron micrographs suggested that the membrane surface area when filopodia were taken into account was $50.3 \pm 5.4\%$ ($n = 14$) greater than the surface area determined from the cell's diameter. This discrepancy suggests that some cells burst, or that the pipette seal ruptured during application of pressure before all the filopodia had flattened out. For this reason, the surface area of HEK-293 cells was estimated by adding 50% to the value calculated from their initial diameter. The corrected surface area was used to calculate C_m, and the results are presented in Table 2.

Despite the large increase in the membrane protein content of transfected HEK-293 cells, there was no detectable difference between C_m measured in transfected and untrans-

TABLE 2 C_m for HEX-293 cells

Cell type	C_m(μF/cm2)
Untransfected cells	1.11 ± 0.08 ($n = 30$)
Transfected cells	1.05 ± 0.09 ($n = 12$)

fected cells. The estimated value of C_m was slightly larger in HEK-293 cells than in neurons, but this discrepancy may reflect a systematic error arising from the indirect estimate of HEK-293 membrane surface area.

DISCUSSION

The value for C_m for neuronal membrane was estimated to be 0.9 μF/cm^2 in three different neuron types from three distinct regions of the central nervous system. These results are in excellent agreement with findings from three mammalian cell lines (0.8 μF/cm^2) (Sukhorukov et al., 1993), from mice mast cells (1.0 μF/cm^2) (Solsona et al., 1998), and from a recent compartmental model study of rat hippocampal interneurons (0.9 μF/cm^2) (Chitwood et al., 1999). In contrast, several recent compartmental studies have suggested values for neuronal C_m ranging from as little as 0.75 μF/cm^2 (Major et al., 1994) to >2 μF/cm^2 (Thurbon et al., 1998). These discrepancies may be due to inaccuracies in the reconstruction of dendritic morphology. Confocal microscopy has shown that conventional fixation and measurement techniques can underestimate the surface area of the soma of adult phrenic motoneurons by 200% (Prakash et al., 1993). The simplifying assumptions needed to construct the compartmental model may also introduce systematic errors. For example, if the membrane resistivity is inappropriately assumed to be uniform, this can introduce errors into the parameter estimates obtained with the compartmental model approach (Clements and Redman, 1989).

In the present study, the diameter of the nucleated patches was measured directly during the electrophysiological recording, thereby avoiding problems with shrinkage during fixation. Furthermore, the spherical geometry of the membrane reduced the requirement for simplifying assumptions and allowed the membrane surface area to be accurately estimated.

Another possible explanation for the reported differences in C_m between different types of neuron is that their membranes may have different protein content (Thurbon et al., 1998). For example, the high density of voltage gated channels in the membrane of squid giant axon produce a voltage-dependent alteration of C_m, although the maximum change observed was only 0.15 μF/cm^2 (Fernandez et al., 1982). Neuronal membrane has a much lower average density of voltage-gated channels than squid giant axon, but contains other proteins that may alter C_m, including a significant density of ligand-gated receptors. Transfection of HEK-293 cells increased the average membrane density of GlyR proteins to a higher level than that found in neurons (Tapia and Aguayo, 1998; Ye et al., 1999). The fraction of the total HEK-293 membrane surface area that would be occupied by GlyR channels can be roughly estimated. The steady-state open probability of homomeric GlyR channels is ~15%, and the conductance of the main open state is 50 pS (Twyman and Macdonald, 1991; Takahashi et al., 1992; Legendre, 1998; Gentet and Clements, in preparation), so ~20,000 GlyR channels were present in a typical transfected HEK-293 cell. Assuming that the GlyR protein has a similar diameter to the homologous nicotinic acetylcholine receptor, which has been measured at ~8 nm (Unwin, 1993), then 20,000 GlyR will occupy ~1 μm^2. This represents only 0.3% of the surface area of a 10-μm-diameter HEK-293 cell. The dielectric constant of proteins has been estimated to range from 2 to 80, compared with a value of only 2 for biological membranes. Even if the maximum dielectric constant of 80 is assumed for the GlyR and other factors are neglected, then transfection would increase C_m by only 12%. However, the hydrophobic transmembrane domain of a ligand-gated channel protein is likely to have relatively few charged or polar residues, so the dielectric constant in this critical region is more likely to be in the range 2–6 (von Kitzing and Soumpasis, 1996), an order of magnitude smaller than the maximum value. In addition, GlyRs are known to have large intracellular and extracellular domains, and the assembled channel protein probably has an hourglass shape (Unwin, 1993), so embedded proteins may increase the average thickness of the membrane. This would reduce C_m, and would tend to counter-balance any increase due to their high dielectric constant. In summary, physiological densities of membrane proteins are unlikely to alter C_m. Consistent with this, expression of membrane protein at or above physiological levels produced no detectable change in C_m in HEK-293 cells.

HEK-293 cells have many fine processes (Fig. 2). The presence of filopodia explains the ability of these cells to expand in response to internal pressure. In contrast, when positive internal pressure was applied to nucleated patches pulled from neurones, the patch always ruptured before any significantly increase in diameter could be observed. This observation suggests that the patch membrane has no fine processes, and that the estimate of nucleated patch surface area determined from Eq. 4 is accurate (see Methods). The membrane surface area of each HEK-293 cell was adjusted to account for the presence of filopodia, before estimating C_m for that cell. A simpler and more direct approach would have been to pull a nucleated patch from these cells, which presumably would have flattened out the fine processes and permitted a direct measurement of surface area. Unfortunately, repeated attempts to pull nucleated patches from HEK-293 cells failed, even after the coverslips were coated with rat tail collagen to ensure that the cells were firmly stuck down. The membrane was not malleable enough to reshape around the large nucleus as the patch electrode was withdrawn. There are several caveats on the 50% correction factor calculated from analysis of electron micrographs. The fixation process may cause shrinkage (Prakash et al., 1993), and may not accurately preserve the cell's morphology. HEK-293 cells were always lifted from the coverslip before commencing electrophysiological recordings. The cells were loosely attached to the coverslip, so this procedure

transiently stressed the cell membrane. This may have altered the number or distribution of fine processes compared with those observed in micrographs. For these reasons, the value of C_m obtained for HEK-293 cells may be less accurate than the values obtained from nucleated patches. Systematic errors of this type would affect the results from transfected and untransfected cells to a similar extent, so comparison of the results from these two groups remains valid.

In summary, we have obtained a C_m of 0.9 μF/cm^2 for three types of neuron, and showed that this value is unlikely to be affected by variations in membrane protein density. This value is in good agreement with C_m values for other mammalian cell types and for artificial bilayers. These findings support the suggestion that C_m is, to a first approximation, a "biological constant."

We thank David Thurbon (JCSMR, Australian National University) for preparing the spinal cord slices used in this study.

This work was supported by an ANU Ph.D. Scholarship (to L.J.G.), a Wellcome Trust Senior Research Fellowship (to G.J.S.), and a Senior Research Fellowship from the Australian Research Council (to J.D.C).

REFERENCES

Bekkers, J. M., and C. F. Stevens. 1991. Excitatory and inhibitory autaptic currents in isolated hippocampal neurons maintained in cell culture. *Proc. Natl. Acad. Sci. USA.* 88:7834–7838.

Chitwood, R. A., A. Hubbard, and D. B. Jaffe. 1999. Passive electrotonic properties of rat hippocampal CA3 interneurones. *J. Physiol.* 515: 743–756.

Clements, J. D., and S. J. Redman. 1989. Cable properties of cat spinal motoneurones measured by combining voltage clamp, current clamp and intracellular staining. *J. Physiol.* 409:63–87.

Cole, K. S. 1968. Membranes, ions and impulses. University of California Press.

Curtis, H. J., and K. S. Cole. 1938. Transverse electric impedance of the squid giant axon. *J. Gen. Physiol.* 21:757–765.

Fernandez, J. M., F. Bezanilla, and R. E. Taylor. 1982. Distribution and kinetics of membrane dielectric polarization. II. Frequency domain studies of gating currents. *J. Gen. Physiol.* 79:41–67.

Furshpan, E. J., S. C. Landis, S. G. Matsumoto, and D. D. Potter. 1986. Synaptic functions in rat sympathetic neurons in microcultures. I. Secretion of norepinephrine and acetylcholine. *J. Neurosci.* 6:1061–1079.

Hodgkin, A. L., and A. F. Huxley. 1952. A quantitative description of membrane current and its application to conduction and excitation in nerve. *J. Physiol.* 117:500–544.

Jack, J. J. B., D. Noble, and R. W. Tsien. 1983. Electric current flow in excitable cells. Oxford Science Publications, London.

Jurman, M. E., L. M. Boland, Y. Liu, and G. Yellen. 1994. Visual identification of individual transfected cells for electrophysiology using antibody-coated beads. *Biotechniques.* 17:876–881.

Legendre, P. 1998. A reluctant gating mode of glycine receptor channels determines the time course of inhibitory miniature synaptic events in zebrafish hindbrain neurons. *J. Neurosci.* 18:2856–2870.

Major, G., A. U. Larkman, P. Jonas, B. Sakmann, and J. J. Jack. 1994. Detailed passive cable models of whole-cell recorded CA3 pyramidal neurons in rat hippocampal slices. *J. Neurosci.* 14:4613–4638.

Niles, W. D., R. A. Levis, and F. S. Cohen. 1988. Planar bilayer membranes made from phospholipid monolayers form by a thinning process. *Biophys. J.* 53:327–335.

Prakash, Y. S., K. G. Smithson, and G. C. Sieck. 1993. Measurements of motoneuron somal volumes using laser confocal microscopy: comparisons with shape-based stereological estimations. *Neuroimage.* 1:95–107.

Rajendra, S., J. W. Lynch, K. D. Pierce, C. R. French, P. H. Barry, and P. R. Schofield. 1994. Startle disease mutations reduce the agonist sensitivity of the human inhibitory glycine receptor. *J. Biol. Chem.* 269:18739–18742.

Rall, W. 1962. Theory of physiological properties of dendrites. *Ann. N.Y. Acad. Sci.* 96:1071–1092.

Solsona, C., B. Innocenti, and J. M. Fernandez. 1998. Regulation of exocytotic fusion by cell inflation. *Biophys. J.* 74:1061–1073.

Sukhorukov, V. L., W. M. Arnold, and U. Zimmermann. 1993. Hypotonically induced changes in the plasma membrane of cultured mammalian cells. *J. Membr. Biol.* 132:27–40.

Takahashi, T., A. Momiyama, K. Hirai, F. Hishinuma, and H. Akagi. 1992. Functional correlation of fetal and adult forms of glycine receptors with developmental changes in inhibitory synaptic receptor channels. *Neuron.* 9:1155–1161.

Tapia, J. C., and L. G. Aguayo. 1998. Changes in the properties of developing glycine receptors in cultured mouse spinal neurons. *Synapse.* 28:185–194.

Thurbon, D., H. R. Luscher, T. Hofstetter, and S. J. Redman. 1998. Passive electrical properties of ventral horn neurons in rat spinal cord slices. *J. Neurophysiol.* 79:2485–2502.

Twyman, R. E., and R. L. Macdonald. 1991. Kinetic properties of the glycine receptor main- and sub-conductance states of mouse spinal cord neurones in culture. *J. Physiol.* 435:303–331.

Unwin, N. 1993. Nicotinic acetylcholine receptor at 9 Å resolution. *J. Mol. Biol.* 229:1101–1124.

von Kitzing, E., and D. M. Soumpasis. 1996. Electrostatics of a simple membrane model using Green's functions formalism. *Biophys. J.* 71: 795–810.

Ye, J. H., R. Schaefer, W. H. Wu, P. L. Liu, V. K. Zbuzek, and J. J. McArdle. 1999. Inhibitory effect of ondansetron on glycine response of dissociated rat hippocampal neurons. *J. Pharmacol. Exp. Ther.* 290: 104–111.